# Enhanced Model-Based Approach of Spacecraft Docking System Simulation

**Tommaso Aresi**[1], **Pierangelo Masarati**[1]

[1] Department of Aerospace Science and Technology
Politecnico di Milano
via La Masa 34, Milano, 20156, Italy
[tommaso1.aresi@mail,pierangelo.masarati@]polimi.it

## ABSTRACT

This paper models a docking system using multibody dynamics, for its integration into algorithms like optimization, guidance, navigation, and attitude determination. The system is described in the International Docking System Standard and aims to simulate docking mechanics, considering more accurate off-nominal situations. Modeling and simulation of the docking process via the finite element method are suitable for detailed mechanical analysis, but balancing the computational efficiency and accuracy required in an integrated design calls for a different approach. This work provides a design tool, taking into account the docking simulation from the early stages.

**Keywords:** Spacecraft Docking.

## 1 INTRODUCTION

Rendez-Vous Docking or Berthing (RVD/B) technology and techniques are used to resupply orbital platforms and stations, switch crews in orbital stations, repair spacecraft in orbit, retrieve and capture spacecraft to bring them back to Earth, and re-join orbiting vehicles from the ground. Docking is the act of two spacecraft joining and sealing to one another with a Guidance Navigation and Control (GNC) system active until the first touch. [1]

It is important to define a proper simulation environment in order to model both the docking dynamics and control logic in the most embedded way between different fields such as GNC design, Attitude Determination and Control System (ADCS) design, Multibody System Dynamics design and Structures and Mechanisms design.

## 2 MULTIBODY MODEL

This paper refers to the IDSS Interface Docking Document (IDSS IDD) [2] guidelines for materials and mass properties of docking system and spacecraft. The system is modeled in MBDyn (`https://mbdyn.org/`) [3, 4], defining multibody entities such as elements (bodies and joints) and nodes.

The system is divided into three body elements: the International Space Station-Hosting Vehicle (HV), the approaching spacecraft-Visiting Vehicle (VV), and the Visiting Vehicle Soft Capture System (SCS). Each element has its own set of properties and parameters that describe its behavior within the system, such as mass, inertia, and geometry.

Structural nodes have *6* degrees of freedom, representing position and orientation in the 3D space, and thus describe the kinematics of rigid-body motion in space. The three bodies are dynamic nodes with inertia that provide linear and angular momenta degrees of freedom. Dummy structural nodes, rigidly connected to the dynamic ones, are used to visualize the kinematics of arbitrary points during the simulation. The modeling was made hierarchically.

A joint is an element that connects, in a prescribed way, different rigid bodies within a multibody system. There are several types of joints available, each with its own set of parameters that define its behavior. Joints may have internal degrees of freedom when they introduce kinematic constraints in form of algebraic relationships between the coordinates of the nodes they connect. By

| **NDSB1** | Guide Petal | SCS Ring | HCS Plane |
|---|---|---|---|
| **Material** | $7075-T7351$ | " | 2219-Al |
| **density**, g/cc | 2.81 | " | 2.84 |
| **Young's Modulus**, GPa | 72 | " | 73.1 |
| **Poisson Ratio**, | 0.33 | " | " |
| **Shear Modulus**, GPa | 26.9 | " | 27.0 |
| **Yield Strength**, MPa | 434 | " | 350 |

Table 1: NDSB1 material properties

| **Vehicles** | $m$, kg | $I_{xx}$, kg·m$^2$ | $I_{yy}$, kg·m$^2$ | $I_{zz}$, kg·m$^2$ |
|---|---|---|---|---|
| **IDSS** | 5000 | $34 \cdot 10^3$ | $18 \cdot 10^3$ | $18 \cdot 10^3$ |
| **SCS** | 40 | 12.67 | 6.42 | 6.42 |
| **HCS** | 300 | 579.4 | 450 | 452 |

Table 2: Visiting vehicles inertia properties

defining the properties of each joint element, and combining them together with the other elements, the system can be fully described. Joint elements used in complex mechanical systems are total joints (selective constrain components of relative displacement and rotation between parts), rods, and deformable displacement joints (establishing relative configuration-dependent forces between parts), allowing for precise control over the motion of connected bodies. The model presents *15* joint elements:

- *6* rods between Hard Capture System (HCS) and SCS, modeling the linear actuator system (LAS);
- *1* driven total joint between SCS and ISS; it clamps the nodes when the mating systems are close enough so that latches strikers impose a constrain along the motion axis;
- *1* driven total joint between HCS and ISS; it clamps the nodes when the mating systems are close enough so that the HCS active and passive hooks constrain the capture system;
- *1* driven total joint imposes the velocity of the HCS node, simulating the Guidance, Navigation, and Control (GNC) system;
- *1* total joint between HCS ans SCS, this imposes a slider between the HCS and SCS, it is then deleted, it is used for preliminary settings to reduce modeling uncertainties;
- *1* total joint between HCS ISS nodes, this imposes a slider between the HCS and SCS, it is then deleted, it is used for preliminary settings to reduce modeling uncertainties;
- *1* total joint on ISS, it clamps the ISS and can be deleted, in a first approximation ISS is not free to move;

The actuation elements are implemented using the prescribed strain, $\varepsilon_p$, of rod elements, namely

$$F = F(\varepsilon - \varepsilon_p, \dot{\varepsilon}) \tag{1}$$

which is formulated according to the control logic of the docking system. Their rather sophisticated constitutive law is implemented in a dedicated user-defined module, a specific docking module with the state machine and control logic, following NASA guidelines. The 6 rods are arranged in a Stewart platform fashion, with 3 couples of hinges on the SCS and 3 couples of mirrored hinges on the HCS.

| | $X$ | $Y$ | $Z$ |
|---|---|---|---|
| **IDSS** | 2.3 | 0 | 0 |
| **SCS** | 0.015 | 0 | 0 |
| **HCS** | 0.165 | 0.356 | 0.0045 |

Table 3: $X$, $Y$, $Z$ coordinates of the capture system mating plane center, m

Joint elements are also used model the contacts. The contact between latch and striker is provided by driving a rod joint element. The contact between the petals is modeled using deformable displacement joints, with instances of the continuous contact module (`cont-contact`) in the direction normal to the surface to model finite contact areas. Contact at an angle with respect to the tangent plane can cause the outgoing velocity and angle to be significant enough to allow the object to fall freely.

The regions in the mating systems where the contact can occur are the edges of the petals and the latches and strikers spots. Given the dimensions of the edge limiting the contact area $a = 0.3$ m and $b = 0.011$ m, given the orientations of each area, the contacts are geometrically well defined. The dimensions on the edges enforce the minimum number of contact points: *30* for each edge for a total of *180* contact points and relative contact joint.

The contacts module requires the characterization of its parameters to model the contact force. The formulation proposed in [5, 6] with restitution coefficient $e_{\text{res}} = 0.6$, stiffness $k_{\text{el}} = 2 \cdot 10^3$, exponent $n = 1.5$ is used.

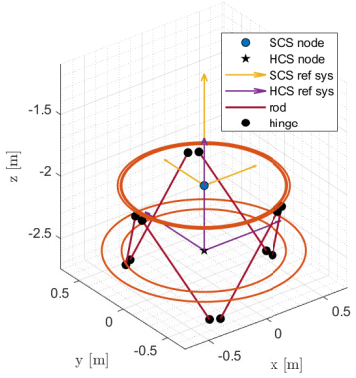


Figure 1: Geometry of the Docking System

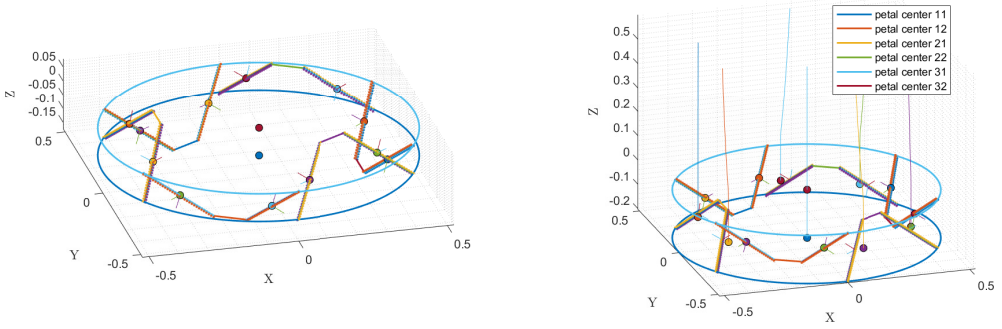


(a) Contact nodes nominal displacement

(b) Contact nodes off-nominal interaction

Figure 2: Contact nodes displacements

## 3 STATES AND CONTROL

This paper simulates the NASA Docking System Block 1 (NDSB1) [7] since it is the standardized docking system developed by NASA for use in various space missions. It uses a "state machine" to represent the system's behavior as a series of states and transitions between those states. The modes or states defined by the state machine are described in NASA documentation and are managed by the Linear Actuator System (LAS). The conditions to trigger the state change are stated below, with each transition requiring to be in the previous state to have a sequential ordering.

The aforementioned defined modes are *7*: *INITIAL*, *EXTRACTION*, *LUNGE*, *ATTENUATION*, *ALIGNMENT*, *RETRACTION*, *STRUCTURAL MATING*.

- The condition to pass from INITIAL to EXTRACTION mode is that the spacecraft overcome a threshold distance, in this simulation, the triggering distance is $d^{\text{sc}}_{\text{extraction}} < 3$ m.
- Any contact between the docking system is required to transition from extraction to lunge mode. This implies accounting for any of the contact joints aforementioned, $\sum_i F_{\text{cont}_i} > 0$.
- The condition to pass from LUNGE to ATTENUATION mode: each latch is engaged to its striker within a certain tolerance, such that $||\mathbf{x}_{\text{latch}_i} - \mathbf{x}_{\text{striker}_i}|| < \text{tol}$, where $\text{tol} = 0.0005$ m.
- The condition to pass from ATTENUATION to ALIGNMENT mode is that the spacecraft's kinetic energy is below a tolerance, $E^{\text{SC}}_{\text{kin}} < \text{tol}$, where $\text{tol} = 0.001$.
- The condition to pass from ALIGNMENT to RETRACTION mode is that each actuator length $l_{\text{LAS}_i}$ is at the prescribed elongation $l_{\text{target}}$ within a strict tolerance, $|l_{\text{LAS}_i} - l_{\text{target}}| < \text{tol}$, where $\text{tol} = 0.01$ m.
- The condition to pass from RETRACTION to STRUCTURAL MATING mode is that the elongation of LAS is small enough to allow structural hooks engagement, such that $|l_{\text{LAS}_i} - l^{\text{SM}}_{\text{target}}| < \text{tol}$ with $l^{\text{SM}}_{\text{target}} = 0.2$ m and $\text{tol} = 0.001$ m.

A new module was written in C++ for MBDyn to manage all states and control laws, as well as define a new driver to drive joints to turn them on and off. The paper proposes a saturated Proportional-Derivative (PD) control on each actuator's displacement and velocity, independent for each actuator, to limit the total force put on the mating ring and structure behind it. This behavior continues until the state machine's trigger for the next phase. An important aspect is that straightforward formulation of NASA guidelines [7, 8, 9] like the one written below can lead to discontinuities in numerical computation.

$$\begin{cases} F = k_p(u - u_{\text{target}}) + k_d(\dot{u} - \dot{u}_{\text{target}}) & \text{if } |F| < F_{\max} \\ F = F_{\max} & \text{if } |F| \geq F_{\max} \end{cases} \tag{2}$$

To address this, scenarios were investigated to find a solution.

1. making use of some linking polynomials all the way up to a finite continuity of class n;
2. to optimize a parametric sigmoid function with the constraints of zeros and slopes, with the goal of minimizing the approximation error;
3. to locate an effective mollifier by making use of the results of Urysohn's lemma.

The first method includes at least $2N(n+1)$ parameters for each of the $N$ discontinuity points (surfaces for higher dimensions) and each of the n continuity classes.

The second strategy's manipulation of the sigmoids did not have enough degrees of freedom to simultaneously recover the slope in the zeros locus and the "time" to reach steady conditions. The new sigmoidal proposed by Liying Cao and other [10] sigmoidal patterns like generalised logistic or Gompertz's function were covered, but they suffer from the aforementioned and coupling parameters. It is useful to stress here the conditions and constraints that such a parametric smooth function shall accomplish:

1. At infinite its behavior shall not differ from the constant behavior of the original piecewise-linear function: $|f(\mathbf{x} \to \infty)| = F_{\max}, \mathbf{k})$.
2. Its value at the discontinuity point shall be tunable: $f(x = \hat{\mathbf{x}}, \mathbf{k}) = \lambda F_{\max}$. Otherwise, an optimality constraint shall be imposed such as minimizing the squared mismatches.
3. Its value should be the same as the value of the original piecewise-linear function in a certain part of the domain (in zero's loci in this case): $f(\mathbf{x} = \mathbf{x}_0, \mathbf{k}) = \tilde{f} = 0$.
4. In the same loci its slope shall be the same as the original piecewise-linear function: $f(\mathbf{x} = \mathbf{x}_0, \mathbf{k})_{|\mathbf{x}} = \boldsymbol{\alpha}$.
5. The cylindrical symmetry condition with respect to the zero's loci line: $f(-(\mathbf{x} - \mathbf{x}_0), \mathbf{k}) = -f((\mathbf{x} - \mathbf{x}_0), \mathbf{k})$.

The third strategy ought to be effective; however, it should make it possible to avoid direct convolution and integration in the software, and it ought to provide directly tunable flexibility.

The application of a linear description, in accordance with Victor M. Jimenez-Fernandez [11] and O. Chua's works [12, 13, 14] , offers an n-dimensional infinite continuity class function with a tunable error that can be managed with just one parameter more than the bare minimum set for piece-wise functions. Ochua canonical representation followed these steps to provide its compact formulation:

- Given $f = f(\mathbf{x})$ with $\mathbf{x} \in \mathbf{R}^n$.
- Defined the *i*th linear partition of $\mathbf{R}^n$ such as $\boldsymbol{\alpha}_i^\top \mathbf{x} = \beta_i$.
- Given the non-degenerate partition of $\mathbf{R}^n$ in $p$ hyperplanes.
- Defined the pseudo-unbounded, essentially-unbounded regions $\mathbf{R}_{j\infty}$ and their amount number $k$.
- Defined two adjacent regions associated with the *i*th hyperplane where their sign-sequence vectors differ only at the *i*th position as $\mathbf{R_{i+}}$ and $\mathbf{R_{i-}}$.

$$\begin{aligned} \mathbf{b} &= \frac{1}{k}\sum_{j=1}^{k} \nabla f(\mathbf{x})\Big|_{\mathbf{R_{j\infty}}} \qquad a = f(\mathbf{0}) - \sum_{i=1}^{p} c_i |\boldsymbol{\beta}_i| \qquad c_i = \frac{1}{2}\frac{\boldsymbol{\alpha}_i^\top (\nabla f(\mathbf{x})|_{\mathbf{R}_{i+}} - \nabla f(\mathbf{x})|_{\mathbf{R_{i-}}})}{\boldsymbol{\alpha}^\top \boldsymbol{\alpha}} \\ f(\mathbf{x}) &= a + \mathbf{b}^\top \mathbf{x} + \sum_{i=1}^{p} c_i |\boldsymbol{\alpha}_i^\top \mathbf{x} - \beta_i| \end{aligned} \tag{3}$$

Victor M. Jimenez-Fernandez's work was used to create a smoothed representation of the standard piecewise-linear model. The result is a differentiable formulation preserving the parameters of the original model, allowing for control of the smoothness grade and approximation accuracy at specific break-point locations.

This notation has overflow problems, which can be solved by using a multi-objective optimization approach. This approach tries to minimize both the approximation error and the governing parameter by utilizing a weighted utopia method. Analytically, it can be useful to understand the relation between the max error $e_{max}$ and $\lambda$, even if a least square method is used.

$$\begin{aligned} A &= a - \sum_{i=1}^{p} c_i \beta_i; \quad B = b + \sum_{i=1}^{p} c_i; \quad C_i = \frac{2c_i}{\lambda}; \quad \hat{B} = B + \sum_{i=1}^{p} c_i \boldsymbol{\alpha}_i; \\ f(\mathbf{x}) &= A + \hat{B}\mathbf{x} + \sum_{i=1}^{p} C_i \log\left(1 + \mathrm{e}^{\lambda(\boldsymbol{\alpha}^\top \mathbf{x} - \beta_i)}\right); \end{aligned} \tag{4}$$

$$e_{max_i} = \frac{2c_i \log(2)}{\lambda_i} = \log(2) C_i; \tag{5}$$

- Given two breaking lines so $p = 2$:

$$\begin{aligned} h_1: &\quad k_1(u-u_0) + k_2(\dot{u}-\dot{u}_0) = -F_{max}; \qquad \boldsymbol{\alpha}_1 = [k_1, k_2]^\top; \quad \beta_1 = -F_{max} + k_1 u_0 + k_2 \dot{u}_0; \\ h_2: &\quad k_1(u-u_0) + k_2(\dot{u}-\dot{u}_0) = F_{max}; \qquad \boldsymbol{\alpha}_2 = [k_1, k_2]^\top; \quad \beta_2 = F_{max} + k_1 u_0 + k_2 \dot{u}_0; \end{aligned} \tag{6}$$

- Given two essentially unbounded regions, $k = 2$
- Defining:

$$\mathbf{R}_{1\infty} = \mathbf{R}_{1-}; \quad \mathbf{R}_{2\infty} = \mathbf{R}_{2+}; \quad \mathbf{R_{1+}} = \mathbf{R_{2-}}; \tag{7}$$

- Computing:

$$f_{|\mathbf{x}}|_{\mathbf{R}_{1-}} = \mathbf{0}; \quad f_{|\mathbf{x}}|_{\mathbf{R}_{1+}} = f_{|\mathbf{x}}|_{\mathbf{R}_{2-}} = [k_1, k_2]^\top; \quad f_{|\mathbf{x}}|_{\mathbf{R_{2+}}} = \mathbf{0}; \tag{8}$$

Given $f(\mathbf{0}) = -\mathbf{F}_{max}$, the canonical representation, with the minimum parameter set, is defined as:

$$\begin{aligned} &\mathbf{b} = \mathbf{0}; \quad c_1 = 1/2; \quad c_2 = -1/2; \\ &a = -F_{max} - \frac{1}{2}|-F_{max} + k_1 u_0 + k_2 \dot{u}_0| + \frac{1}{2}|F_{max} + k_1 u_0 + k_2 \dot{u}_0|; \end{aligned} \tag{9}$$

$$\begin{aligned} f(\mathbf{x}) = \Big\{ &-F_{\max} - \frac{1}{2}(|k_1 u_0 + k_2 \dot{u}_0 - F_{\max}| + |k_1 u_0 + k_2 \dot{u}_0 + F_{\max}| + \\ &+ |k_1(u-u_0) + k_2(\dot{u}-\dot{u}_0) + F_{\max}| - |k_1(u-u_0) + k_2(\dot{u}-\dot{u}_0) - F_{\max}|) \Big\}; \end{aligned} \tag{10}$$

It is now provided the actual implemented non-linear control law:

$$\begin{aligned} &A = -\frac{1}{2}|-F_{\max} + k_1 u_0 + k_2 \dot{u}_0| + \frac{1}{2}|F_{\max} + k_1 u_0 + k_2 \dot{u}_0|; \\ &\hat{\mathbf{B}} = \mathbf{0}; \quad C_1 = 1/\lambda; \quad C_2 = 1/\lambda; \end{aligned} \tag{11}$$

$$\begin{aligned} f(\mathbf{x}) = \Big\{ &|k_1 u_0 + k_2 \dot{u}_0 + F_{\max}| - \frac{1}{2}\left(|k_1 u_0 + k_2 \dot{u}_0 - F_{\max}| + \frac{1}{\lambda}\log\left(1 + \mathrm{e}^{-\lambda(k_1(u-u_0) + k_2(\dot{u}-\dot{u}_0) + F_{\max})}\right) + \right. \\ &\left. - \frac{1}{\lambda}\log\left(1 + \mathrm{e}^{-\lambda(k_1(u-u_0) + k_2(\dot{u}-\dot{u}_0) - F_{\max})}\right)\right) \Big\}; \end{aligned} \tag{12}$$

For a two-dimensional control law, the number of parameters of this formulation is the minimum one, just six: $F_{\max}$, $u_0$, $\dot{u}_0$, $\alpha_1 = \alpha_2 = \alpha$, $k_1$ and $k_2$.This function is tunable and respects all constraints. It adds one parameter, $\alpha$, to enforce infinite order smoothness, while selecting a linking polynomial for continuity implies ten more parameters in one dimension. With this control law tuned for each docking mode, it implies 70 more than the already required seven parameters.

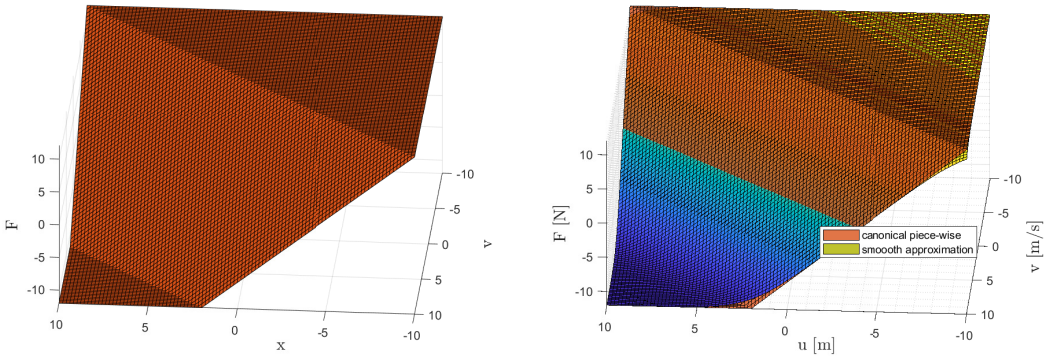


(a) Control law directly from NASA (b) Control law after smoothing process

Figure 3: Dummy control laws for understanding

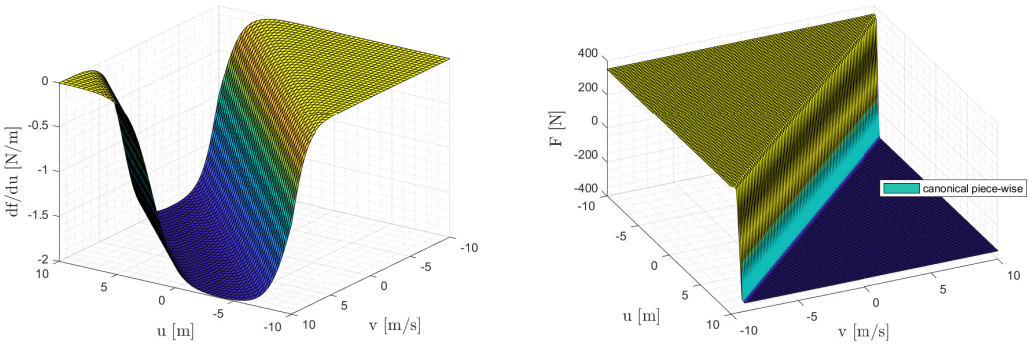


(a) First derivatives along position (b) Implemented control law

Figure 4: Derivatives and actual control law

Another result is the formulation of a new one-dimensional sigmoidal function that can overcome the issues of Liying Cao and colleagues, the *tanh* expression, and the generalized logistic function. It provides the smallest possible group of parameters and decoupled parameters, making the initial guess more guessable and the process of optimizing the data fit more simple.

$$x_1 = \frac{F_1}{m} + x_0; \quad x_2 = \frac{F_2}{m} + x_0; \tag{13}$$

$$f(x) = F(0) + \frac{m}{2}\left(-|x_1| + |x_2| + x_1 - x_2 + \frac{2}{\alpha_1}\log\left(1+\mathrm{e}^{-\alpha(x-x_1)}\right) - \frac{2}{\alpha_2}\log\left(1+\mathrm{e}^{-\alpha(x-x_2)}\right)\right)$$

Where there are just six parameters, $F_1$ for the lower asymptote, $F_2$ for the upper asymptote, $m$ for the slope in $x_0$, $x_0$ the zero passing point and $\alpha_1$ and $\alpha_2$ complying for the curvature in the slope change points. If symmetry is imposed and required just three remain, $F$, $m$, $\alpha$.

The PD controller is no longer fully actuated, leading to saturation behavior and difficult parameters characterization. To overcome these troubles, it is suggested to start the modeling with a normal PD controller and then tune it with NASA guidelines. The control parameters required for this docking modeling are listed below.

| STATE | $k_1$ N/m | $k_2$ Ns/m | $\lambda$ n.d. | $F_{max}$ N | $u_0$ m | $\dot{u}_0$ m/s |
|---|---|---|---|---|---|---|
| **EXTRACTION** | 2000 | 200 | 0.02 | 200 | 0.3 | 0 |
| **LUNGE** | 20 | 2000 | 0.02 | 67 | 0.4 | 0.1016 |
| **ATTENUATION** | 20000 | 50 | 0.02 | 356 | 0.05 | 0 |
| **ALIGNMENT** | 6000 | 5850 | 0.001 | 200 | state machine | 0 |
| **RETRACTION** | $4 \cdot 10^6$ | $4.4 \cdot 10^6$ | 0.0001 | 1200 | state machine | 0 |

Table 4: Control parameters

## 4 SIMULATIONS

Here are presented the results of this modeling, the incoming velocity to the target is $v = 0.0368$ in the approaching direction. Different masses are simulated from 300 kg to 5000 kg and a first off-nominal characterization is provided by tilting the incoming spacecraft by 2 degrees with respect to the $\hat{x}$ axis, the incoming direction. The simulations constrain the bodies HCS SCS to keep relative alignment by imposing a total joint and addressing all the motion to the chaser vehicles. Further developments shall overcome these limitations. Simulations are all presented with the same control parameters, to stress their performances and ranges, to follow the ultimate goal to develop a general tool. This shall change in a more detailed simulation where fine adjustment shall be performed, in this situation the customizability of the module and MBDyn, in general, allows a more precise control parameters definition.

The first two plots show the approaching direction in the nominal situation, simulating the mass of the system alone ($300kg$), from the point of view of the vehicle flying to the space station and from the relative displacement of the actuator. The results show a position profile that makes clear the full docking achievement. Simulating different weights with the same control can easily bring uncontrolled situations, fortunately, this has not happened, since the control is robust enough.

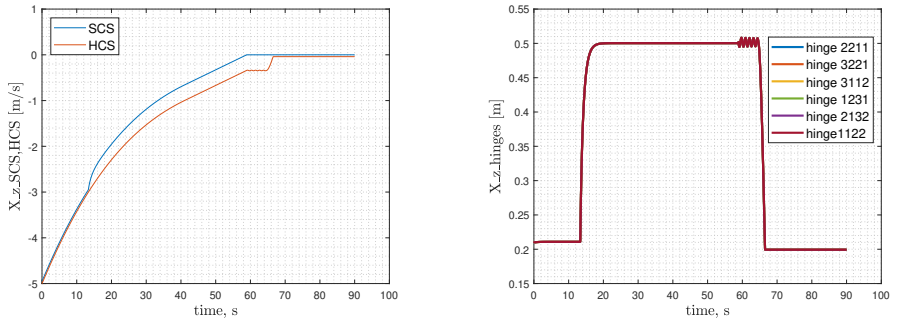


(a) HCS and SCS pos. along incoming axis (b) Relative motion of all actuators

Figure 5: Positions for nominal 300 kg simulation

Below are shown the actuators' control forces and relative velocities. Even if the forces are embedded with respect to the prescribed forces stated by NASA, it shall address that in this light configuration, forces oscillate a lot and it can become an issue to overcome. Velocities are quite low everywhere, there are oscillations but they do not have a wide excursion.

The off-nominal situation in general, with the plot of the positions, shows that even in this situation the simulation provides good results and the docking is achieved, and zoom over the attenuation mode is provided, it is an important moment where the system is highly stressed and differences between nominal and off-nominal are more visible.

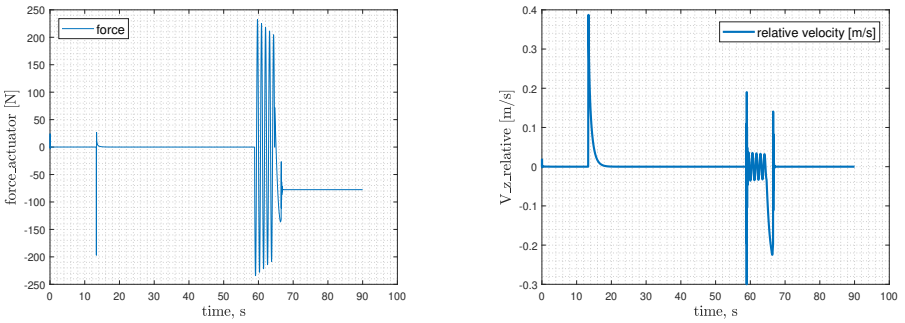


(a) Actuator force (b) Actuator relative velocity

Figure 6: Force and velocity for 300 kg nominal simulation

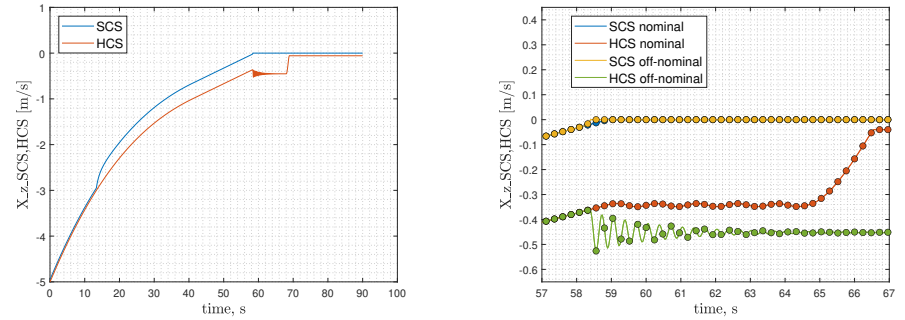


(a) 300 kg off-nominal HCS and SCS displ. (b) Zoom & comparison in atten. mode

Figure 7: Off-nominal general behavior and comparison with nominal simulation

The 5000 kg configuration is presented below, it is already in the off-nominal situation and without the constraint on the spacecraft path, increasing its generality. The plots still show the docking obtained. The comparison with the off-nominal with 300 kg.

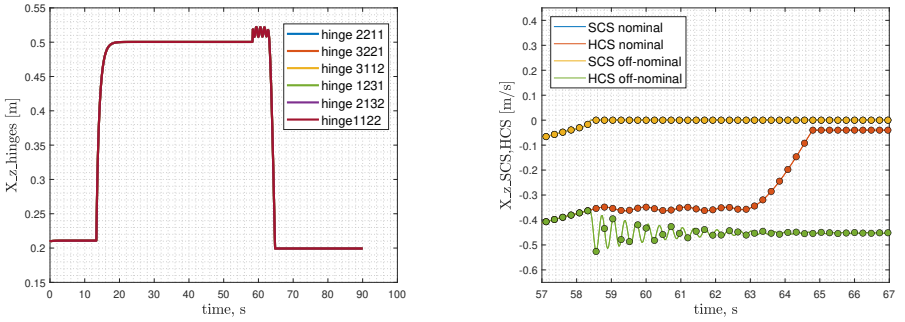


(a) Relative actuator displacements (b) Comparison between different masses

Figure 8: Off-nominal, 5000 kg simulation

## 5 CONCLUSIONS

Further analysis shall be addressed to let the presented system general enough to be implemented autonomously in different algorithms, here are presented some issues to be overcome in future works. A more automatic system to set the control parameters should be defined since even if the work in this paper makes the number of control parameters the fewest as possible while smoothing and respecting NASA guidelines for control, their number still does not allow for an easy way to

select them.

The model and its simulations are still relatively simple. It is missing the full petal contact description, and the spacecraft's motion is still constrained to be nominal besides some tilting on the $\hat{x}$ axis that provides a first off-nominal. Overcoming these issues provides a more reliable tool for simulating control or determining navigation trajectories. The solution to these problems shall be recovered in a new control parameters characterization and in a more detailed contact description.

This work provides a first tool for analysis, with its computational velocity the motion can be simulated in a promising way for embedded analysis, it already simulates with some off-nominal. The NASA control laws are followed in their principal aspects while reducing their complexity still can be adopted for a preliminary analysis.

## REFERENCES


[1] Fehse, W.: Automated Rendezvous and Docking of Spacecraft. Cambridge University Press, Cambridge (2003) doi:10.1017/CBO9780511543388.

[2] kelly, S.M., P., C.S.: International docking system standard (IDSS) interface definition document (IDD). Technical report, NASA (2016)

[3] Masarati, P., Morandini, M., Mantegazza, P.: An efficient formulation for general-purpose multibody/multiphysics analysis. J. of Computational and Nonlinear Dynamics **9**(4) (2014) 041001 doi:10.1115/1.4025628.

[4] Zhang, H., Zhang, R., Zanoni, A., Masarati, P.: Performance of implicit A-stable time integration methods for multibody system dynamics. Multibody System Dynamics **54**(3) (2022) 263–301 doi:10.1007/s11044-021-09806-9.

[5] Flores, P., Machado, M., Silva, M.T., Martins, J.M.: On the continuous contact force models for soft materials in multibody dynamics. Multibody System Dynamics **25**(3) (March 2011) 357–375 doi:10.1007/s11044-010-9237-4.

[6] Stronge, W.J.: Impact Mechanics. 2 edn. Cambridge University Press, Cambridge (2018) doi:10.1017/9781139050227.

[7] (Anonymous): NASA docking system (NDS) interface definitions document (IDD). Technical report, NASA (2016)

[8] Motaghedi, P., Ghofranian, S.: Feasibility of the SIMAC for the NASA docking system. In: AIAA Space and Astronautics Forum and Exposition (SPACE 2014), San Diego, CA, USA (2014)

[9] Dick, B.N., Oesch, C., Rupp, T.: Linear actuator system for the nasa docking system. In: European Space Mechanisms and Tribology Symposium, Hatfield, Hertfordshire, UK (2017)

[10] Cao, L., Shi, P.J., Li, L., Chen, G.: A new flexible sigmoidal growth model. Symmetry **11**(2) (2019) doi:10.3390/sym11020204.

[11] Jimenez-Fernandez, V.M., Jimenez-Fernandez, M., Vazquez-Leal, H., Muñoz-Aguirre, E.: Transforming the canonical piecewise-linear model into a smooth-piecewise representation. SpringerPlus **5**(1) (2016) doi:10.1186/s40064-016-3278-y.

[12] Kahlert, C., Chua, L.O.: The complete canonical piecewise-linear representation. Technical Report UCB/ERL M89/32, EECS Department, University of California, Berkeley (Mar 1989)

[13] Chua, L.O., Ying, R.L.P.: Canonical piecewise-linear analysis. IEEE Transactions on Circuits and Systems **30**(3) (1983) 125–140 doi:10.1109/TCS.1983.1085342.

[14] Chua, L.O., Deng, A.C.: Canonical piecewise-linear representation. IEEE Transactions on Circuits and Systems **35**(1) (Jan 1988)